

H₂-HI Transition and Star Formation in CO-Rich Early-Type Galaxies: Observations meet Theory

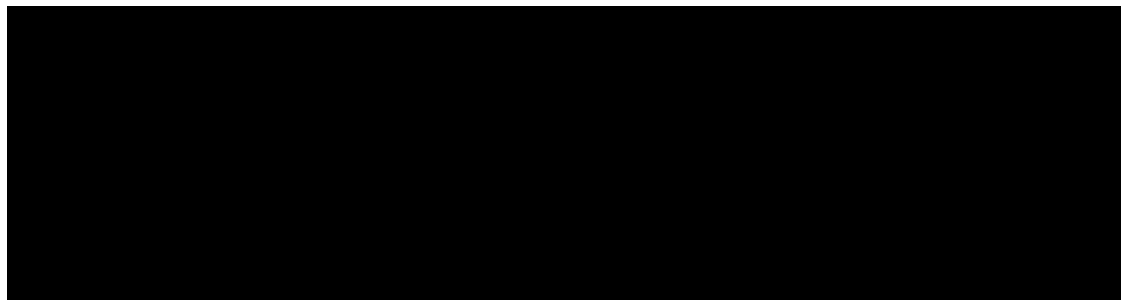
Danielle M. Lucero
SARChI Postdoctoral Fellow
University of Cape Town

Lisa Young (New Mexico Tech)

This work is supported by NSF grant AST-0507432

Motivation

- It is well known that many early-type galaxies (E and S0) contain significant amounts of cold gas and detectable star formation
 - (e.g. Wiklind et al. 1995; Young 2002; Welch & Sage 2003; Sage & Welch 2006; Morganti et al. 2006; Sage et al. 2007; Combes et al. 2007; Osterloo et al. 2007; Alighieri et al. 2007; Welch et al. 2010; Serra et al. 2011, Young et al 2011).
- ATLAS 3^D ----> Multi-wavelength observations of a statistically well defined sample of 260 early-type galaxies derived from the 2MASS all sky survey (out to 42 Mpc; $M_K \leq 21.5$).
 - HI (WSRT 45'') and CO (CARMA 5'') maps.
 - HI maps at too low a resolution to study radial comparisons of H₂ versus HI.



Motivation

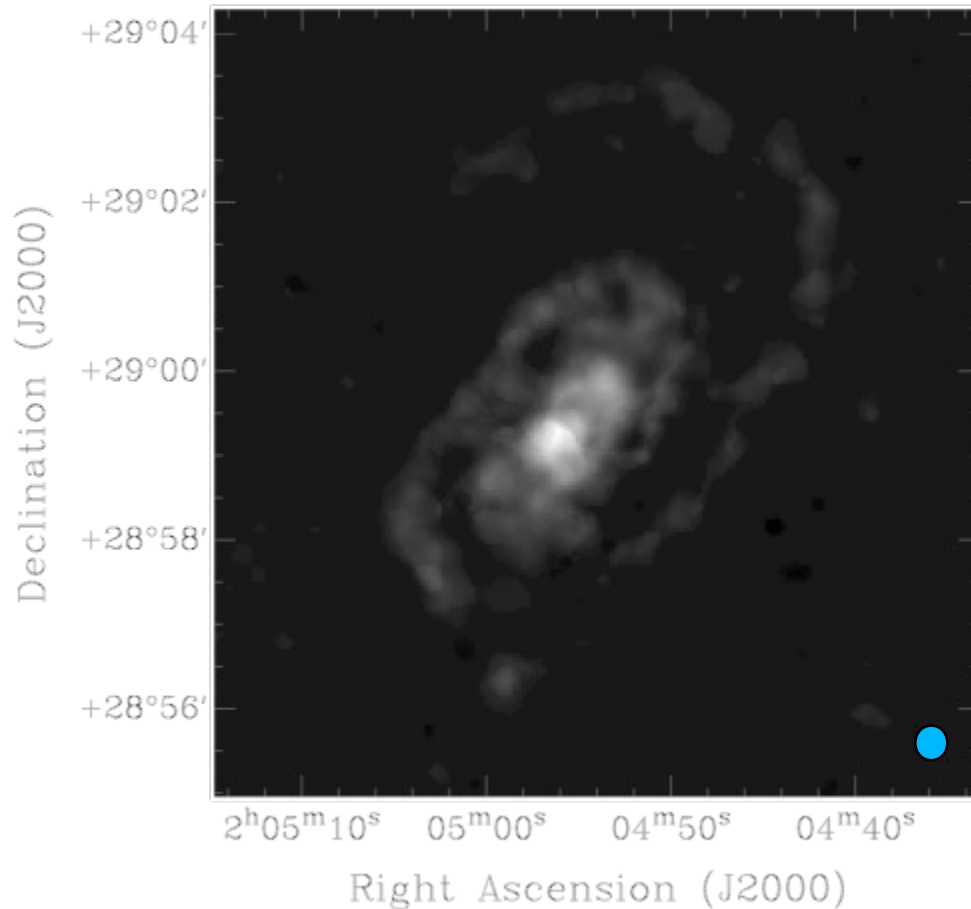
- It is well known that many early-type galaxies (E and S0) contain significant amounts of cold gas and detectable star formation.
- The evolutionary pathway of early-type galaxies is thought to be driven in part by the acquisition and transformation of this cold gas into new stars. To the best of our knowledge stars form only from the molecular gas phase. Clearly, knowledge of the amount of cold gas in the molecular phase versus the atomic phase is an important constraint for theoretical models of star formation and galaxy evolution.
- Use the cold gas kinematics and gas morphologies to look for origins for the HI and CO (Lucero & Young Submitted).
- Test theoretical and empirical models of star formation known for spirals. Is there evidence of star formation where star formation models predict it to occur?
- Test theoretical and empirical models of molecule formation observed for spirals.

Sample and Observations

- Eleven of the most CO-rich early-types (M_{H_2} 6×10^8 - $5 \times 10^9 M_{\text{sol}}$).
- A range of morphologies (6 S0, and 5 E), distances (up to 80 Mpc), environments (field/cluster/group), and optical luminosities ($-21.7 \leq M_B \leq -18.3$).
- All sample galaxies have $R^{1/4}$ classifications as E, E/S0 or S0 in several catalogs.
- Prior knowledge of amount and location of star formation for all sample galaxies (Young, Bendo, Lucero 2009; Lucero & Young 2007).
- HI VLA C array data (15'') are compared to the existing CO maps (7''). HI observations have 2 to 16 times better resolution than the current HI surveys (e.g. ATLAS 3D). Lucero & Young Submitted.

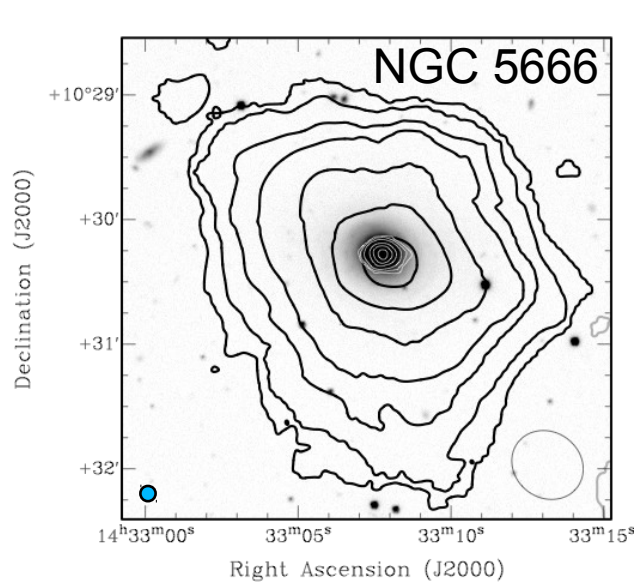
Results

NGC 807

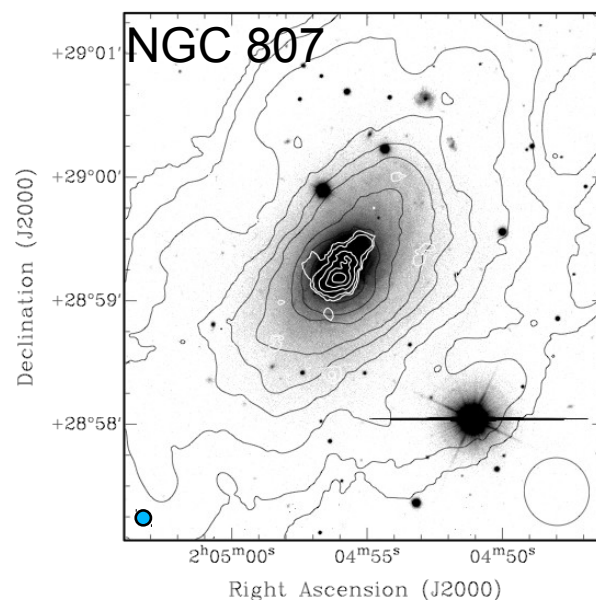


Lucero & Young Submitted

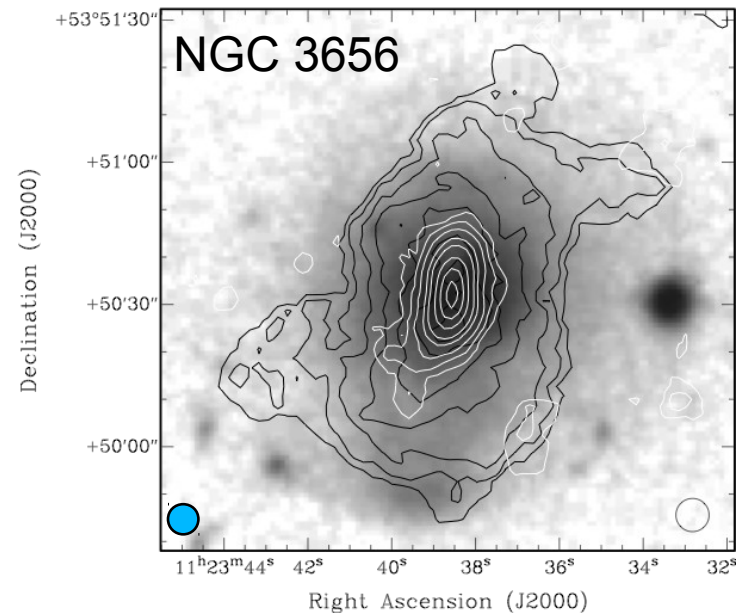
- Five Detections: NGC 3656, NGC 5666, NGC 807, NGC 3032, and UGC 1503 (2 E's and 4 lenticulars).
- One marginally detected in the VLA data: NGC 4150.
- NGC 2320 has an narrow absorption feature redshifted ~ 60 km/s with respect to the systemic velocity.
- Four non-detections ($< \text{few} \times 10^{19} \text{ cm}^{-2}$): NGC 83, NGC 4476, NGC 4526 NGC 4459. All are cluster/group galaxies.



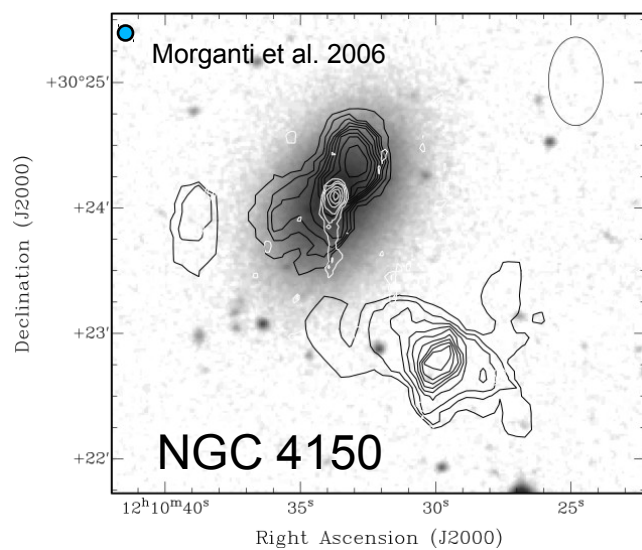
peak HI surface density is $9.1 \times 10^{20} \text{ cm}^{-2}$



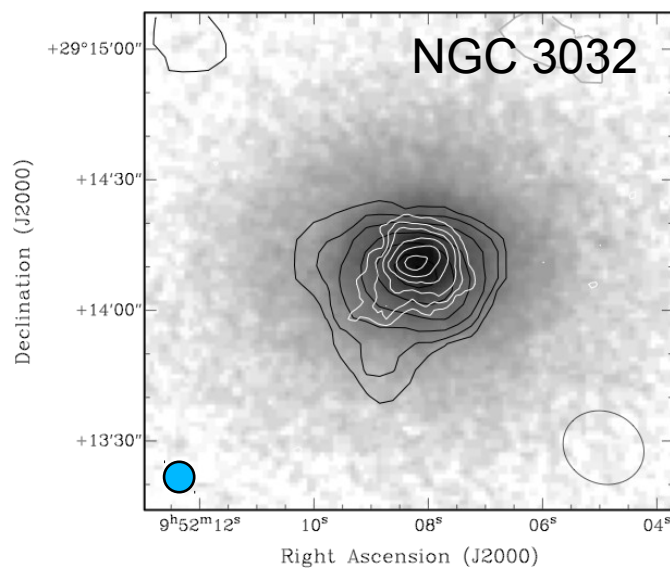
peak HI surface density is $7.7 \times 10^{20} \text{ cm}^{-2}$



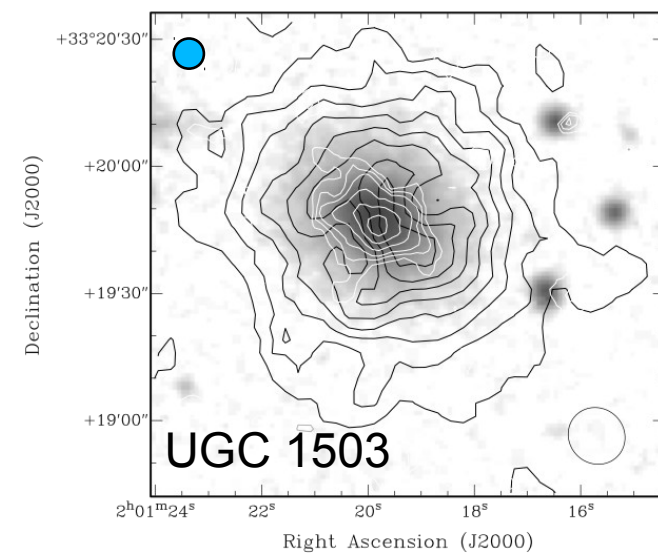
peak HI surface density is $7.2 \times 10^{21} \text{ cm}^{-2}$



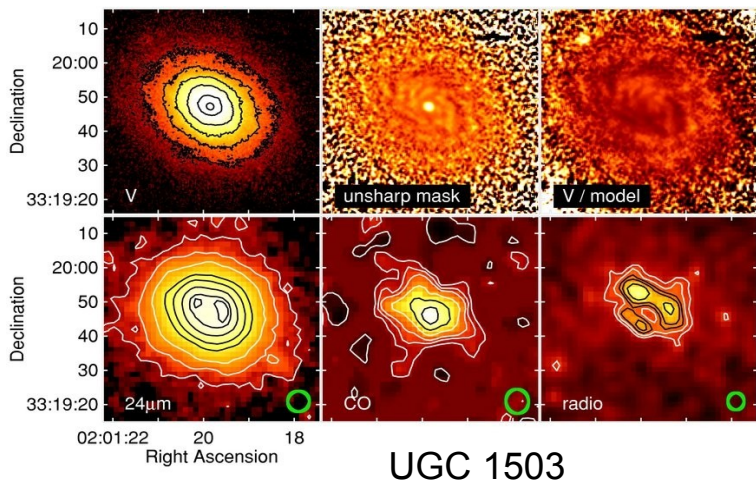
peak HI surface density is $2.9 \times 10^{19} \text{ cm}^{-2}$



Peak HI surface density is $1.3 \times 10^{21} \text{ cm}^{-2}$

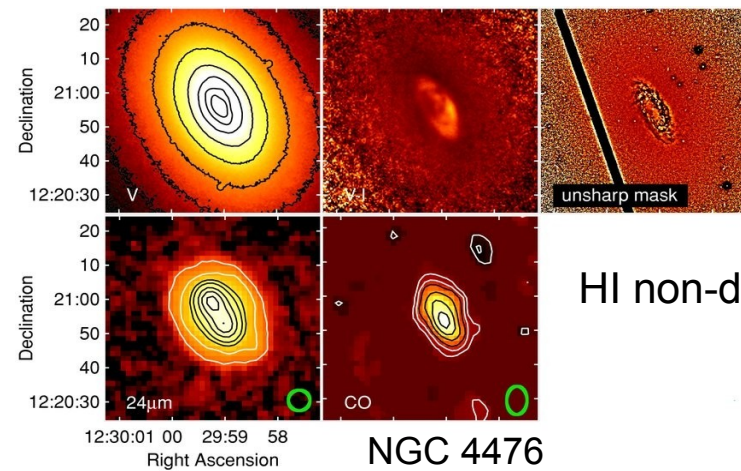


peak HI surface density is $9.9 \times 10^{20} \text{ cm}^{-2}$



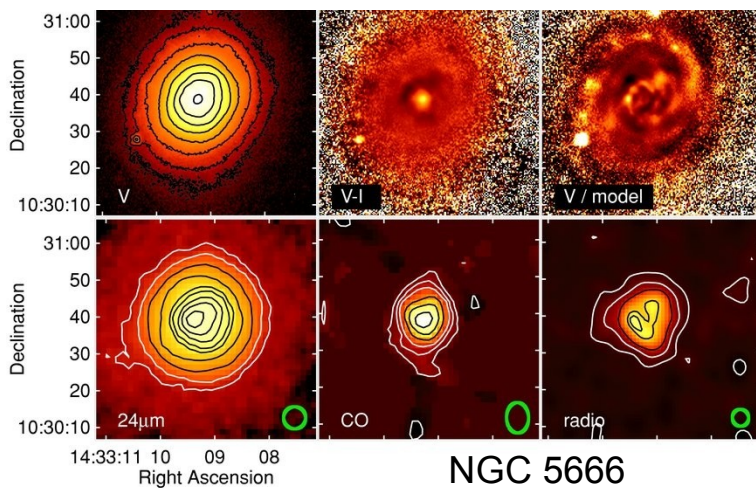
UGC 1503

HI detected

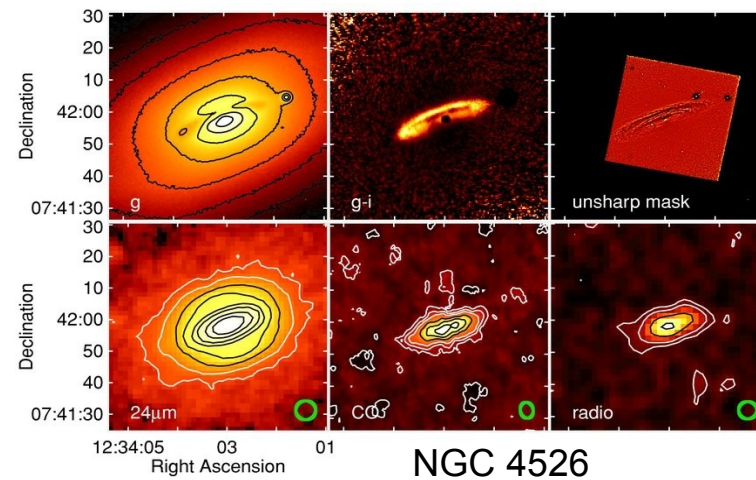


NGC 4476

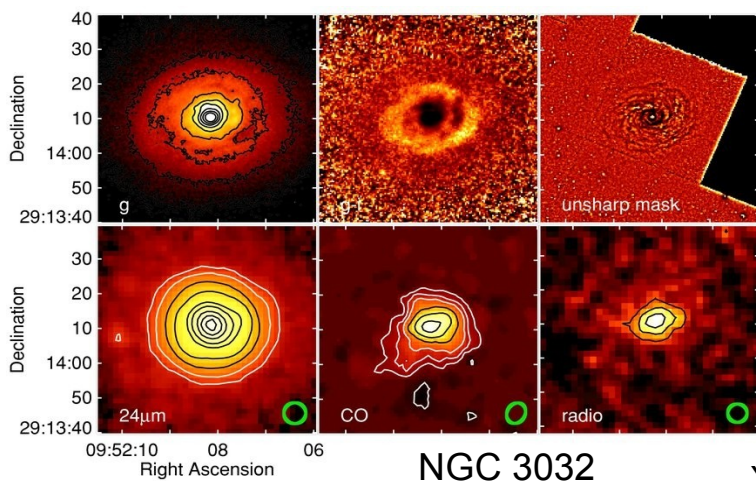
HI non-detected



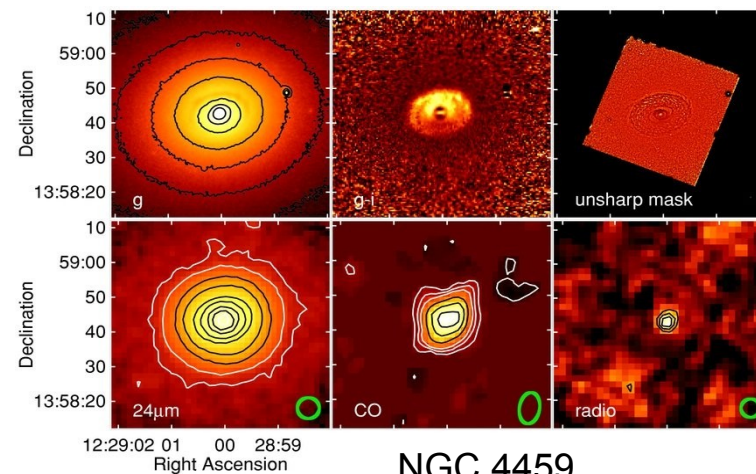
NGC 5666



NGC 4526

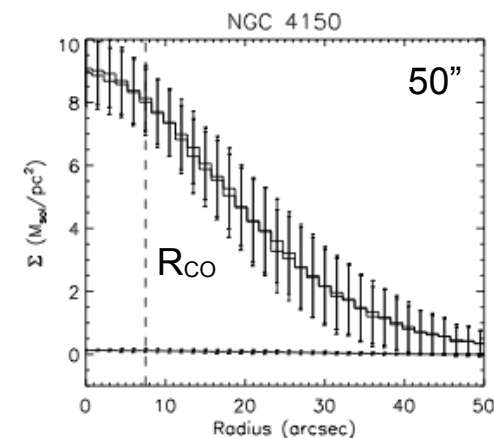
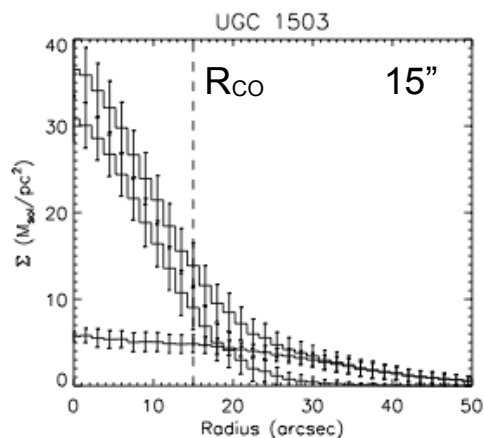
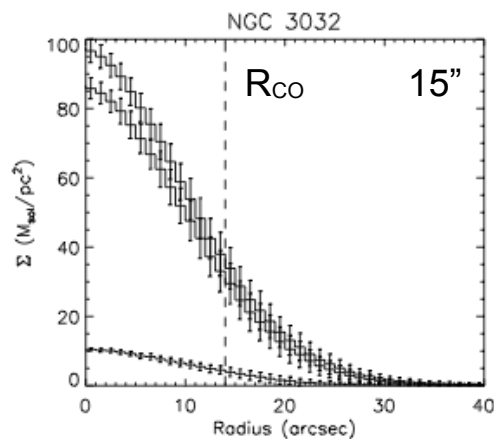
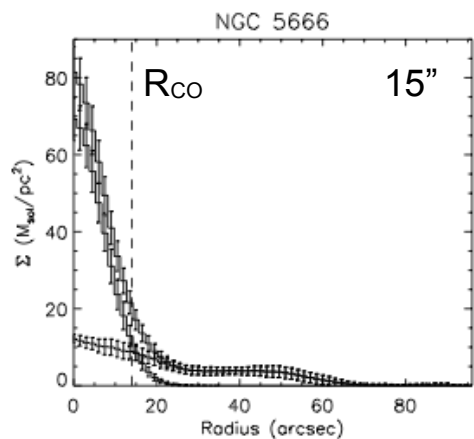
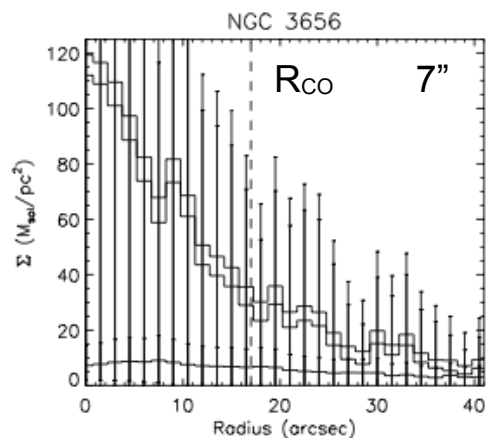
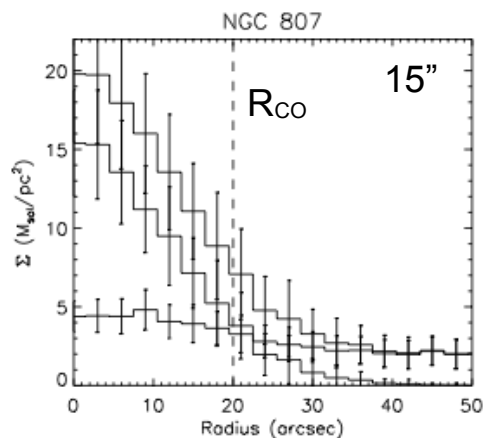


NGC 3032



NGC 4459

Σ_{tot} , Σ_{H_2} , Σ_{HI} Versus Radius



Green: HI surface density
 Black: H₂ surface density
 Orange: HI+H₂ surface density

- Σ_{HI} does not saturate above $9-10 M_{\odot} \text{ pc}^{-2}$ for any of the sample galaxies.

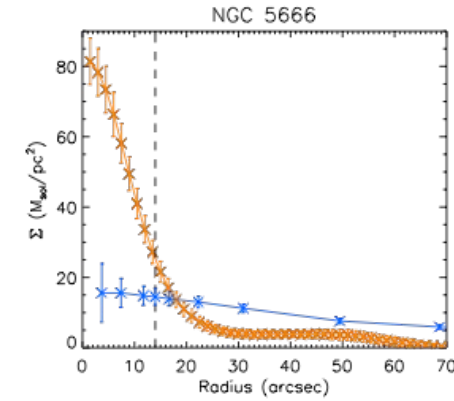
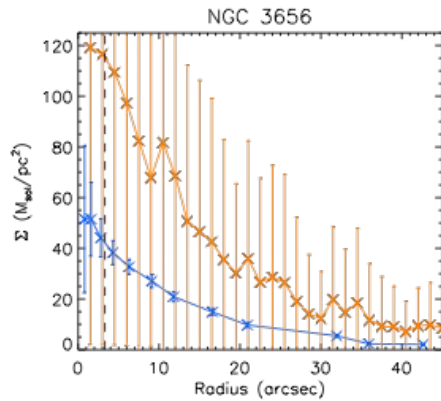
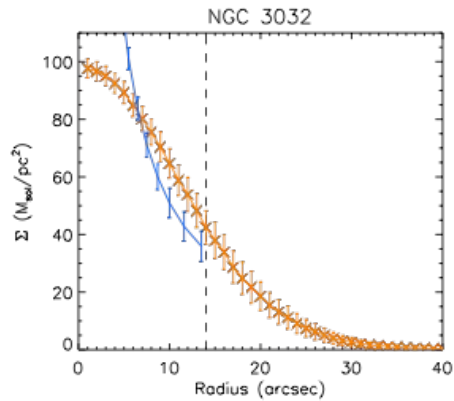
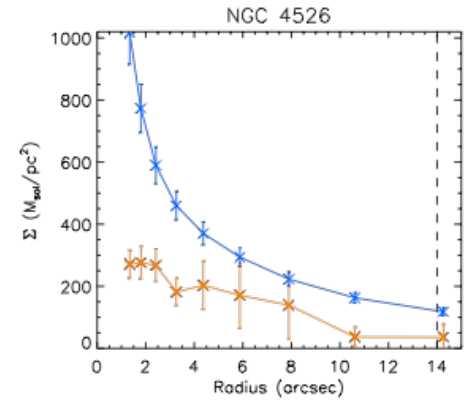
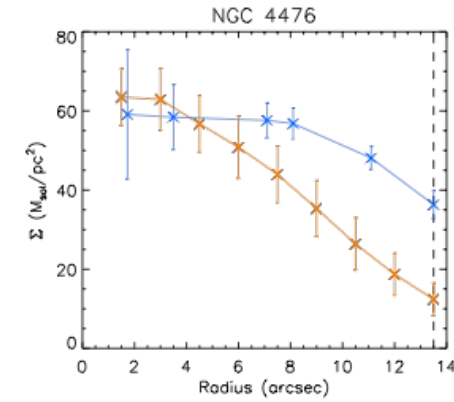
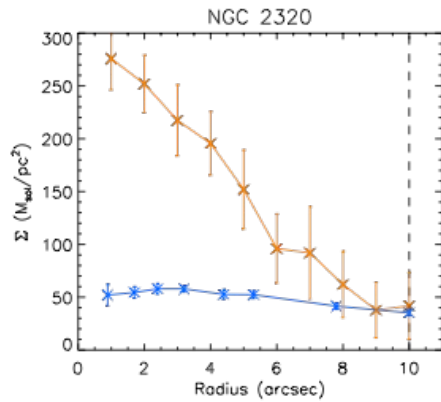
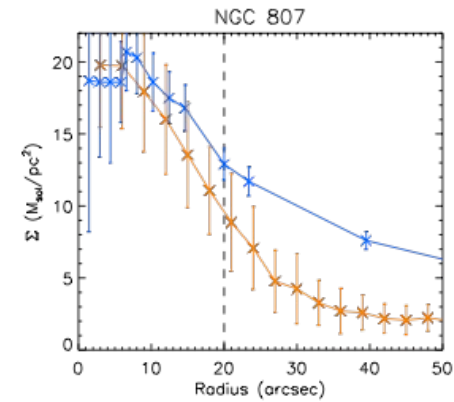
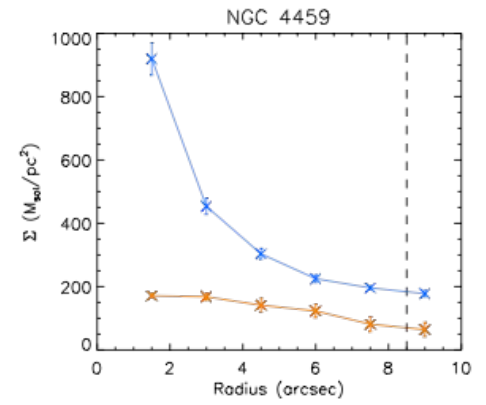
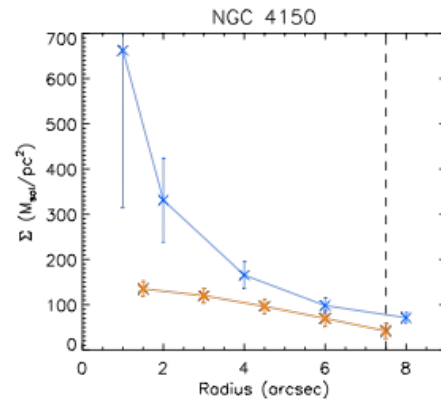
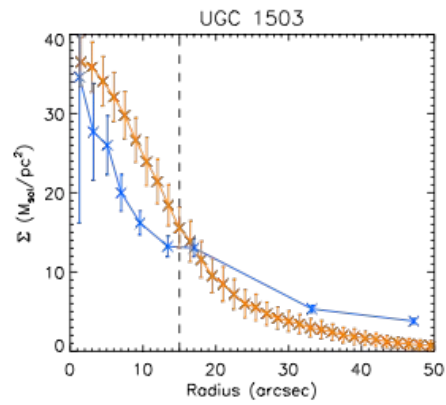
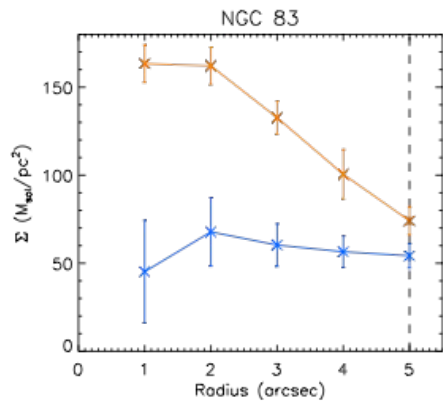
- Σ_{HI} saturation occurs near R_{CO} except for NGC 3032.

- NGC 4150 has extremely low Σ_{HI} throughout.

- Field E's (NGC 807, UGC 1503) saturate at $\sim 5 M_{\odot} \text{ pc}^{-2}$ whereas the field S0's (NGC 3032, NGC 3656, NGC 5666) saturate at $\sim 9-10 M_{\odot} \text{ pc}^{-2}$.

□ Morphological correlation or resolution effects?.

Σ_{crit} Versus Σ_{tot}

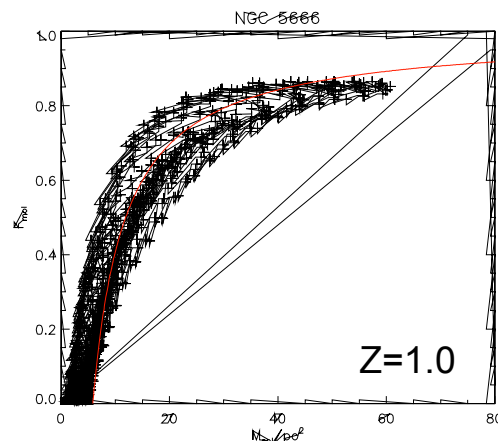
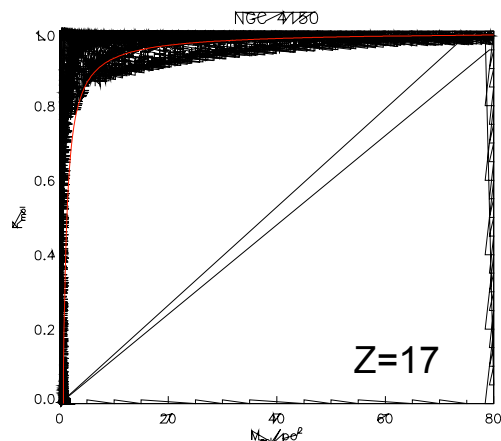
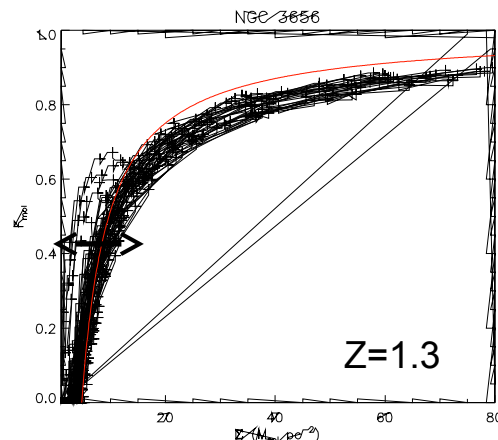
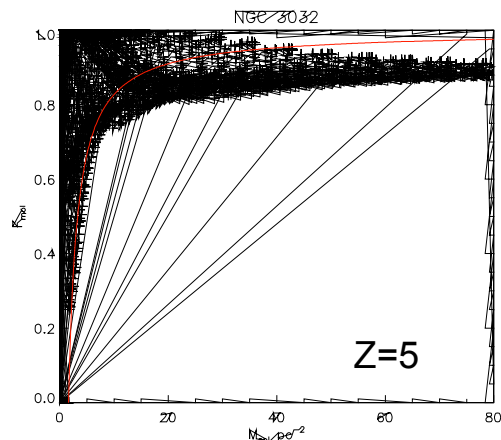
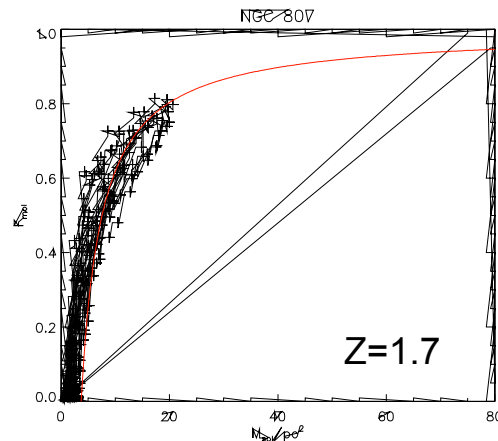
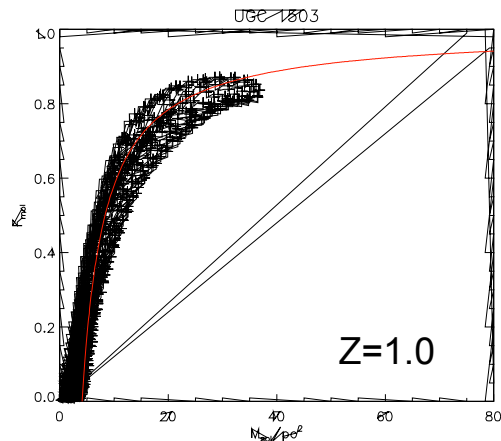


$$Q_g = \frac{\kappa \sigma_g V}{\pi G \Omega \Sigma_{\text{gas}} R} < 1$$

$$\Sigma_{\text{gas}} = \frac{\kappa \sigma_g V}{\pi \Omega G Q_g R}$$

Martin & Kennicutt 2001

The Molecular Fraction: HI Detected Early-Types



----- Krumholz et al. 2009 model

Model assumptions:

$$\zeta't=G'0$$

$$Z'd=Z'g=Z'$$

➤ May not hold in Early-Types

Fit Parameters:

$\text{Log}_{10}(Z)=\langle[\text{Fe}/\text{H}]\rangle = -0.2 \text{ to } 0.4$
(e.g. Kuntschner et al. 2010)

$$\phi_{\text{mol}}=10; \phi_{\text{CNM}}\sim 10$$

NGC 3032 and NGC 4150: High F_{mol} at low Σ_{tot}

➤ Both galaxies show indications of recent interactions or gas accretion!

R_{mol} -Pressure Relation

Recall that Elmegreen's (1993) model predicts:

$$F_{\text{mol}} \propto P^{2.2} j(Z)^{-1}$$

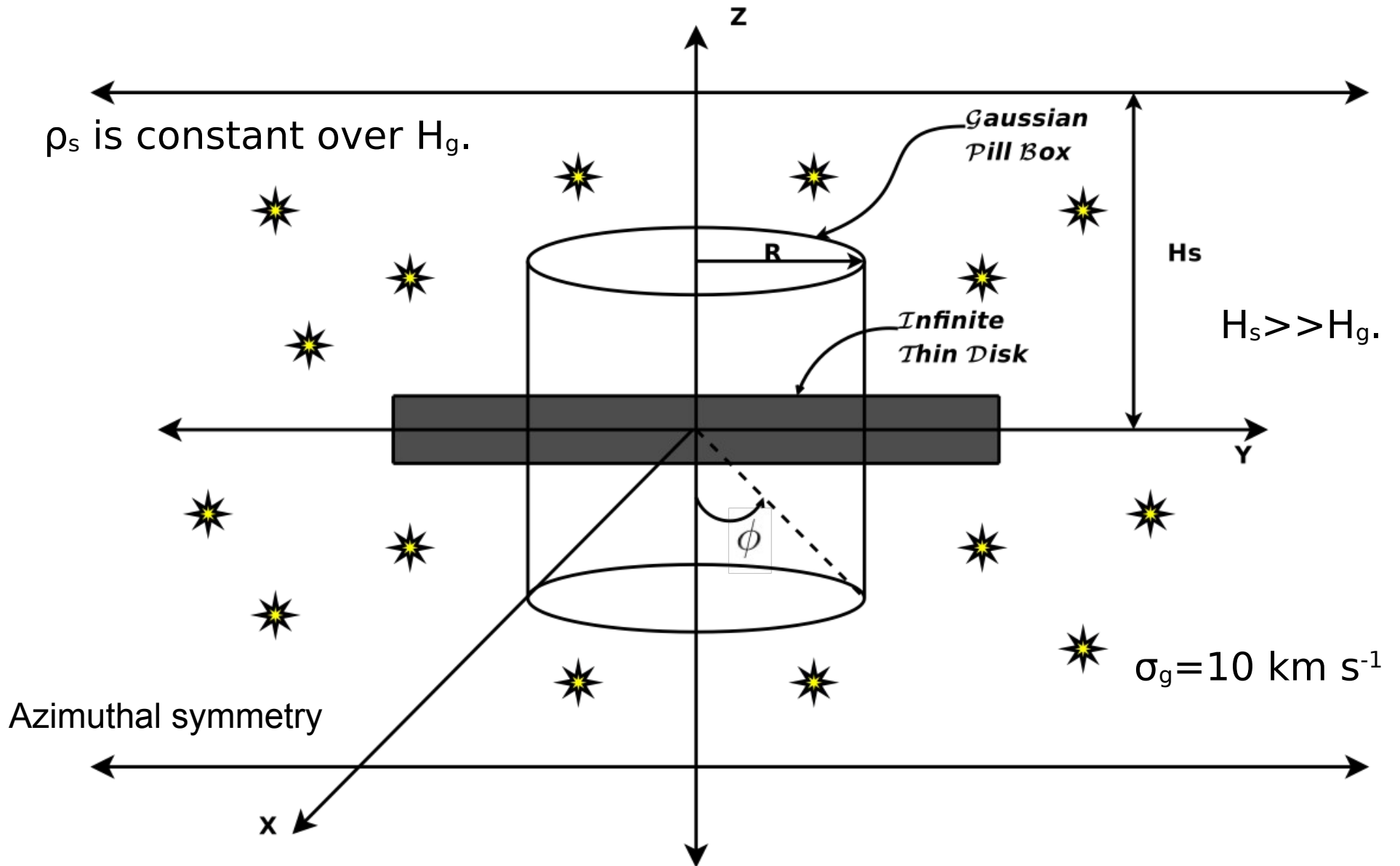
- Several studies of the HI and H₂ maps of nearby spiral galaxies find that the molar fraction, R_{mol} , is a tight function of the midplane hydrostatic pressure (Blitz & Rosolowsky 2004, 2006; Leroy et al. 2008)
- Blitz & Rosolowsky (2006) specifically find:

$$R_{\text{mol}} = P^{0.92}$$

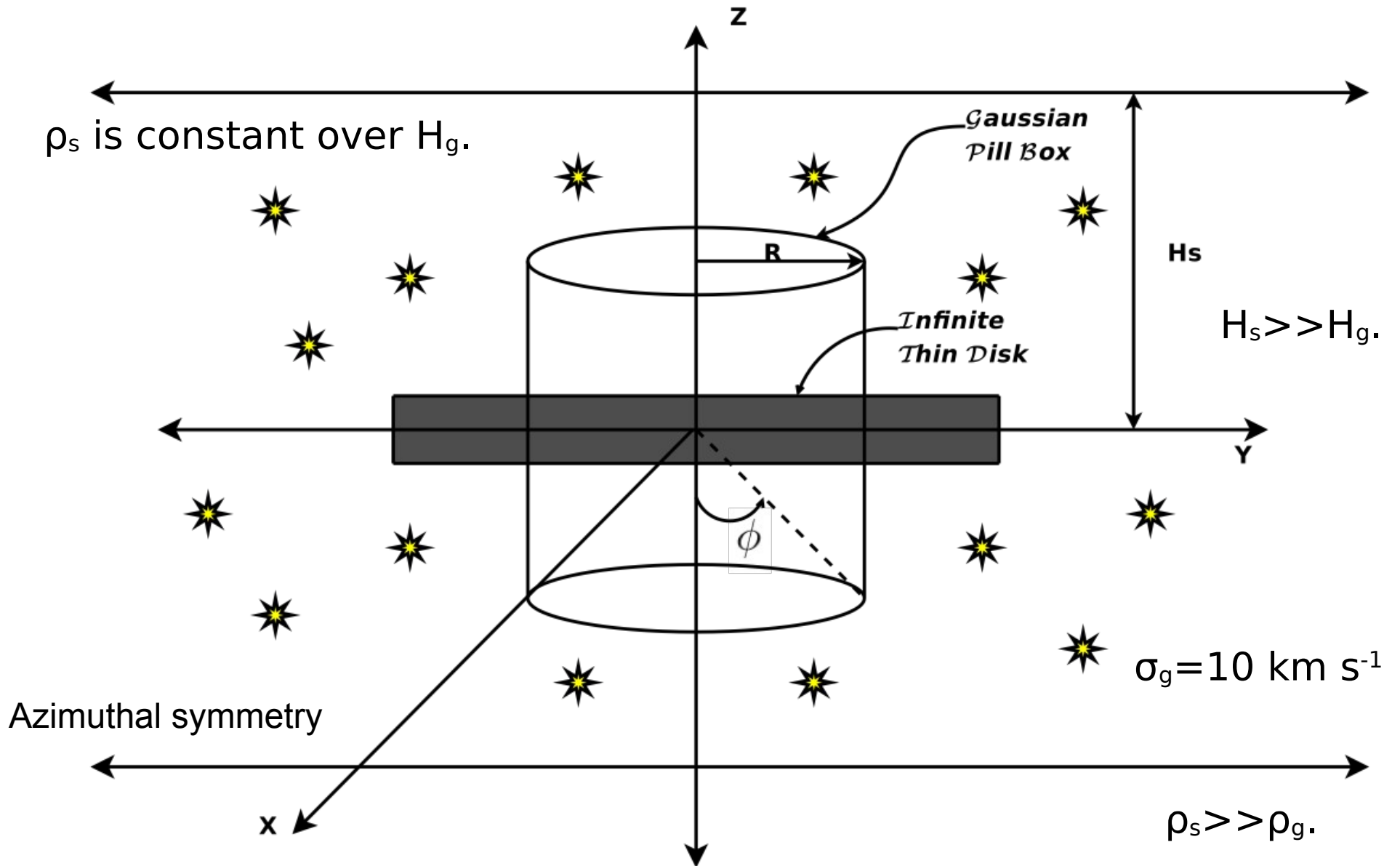
where

$$R_{\text{mol}} = \frac{\Sigma_{\text{H}_2}}{\Sigma_{\text{HI}}}$$

- The $j(Z)$ dependence is assumed to be subsumed into this empirical relationship.



$$P(0) = \rho_g(0)\sigma_g^2 = (2G)^{0.5}\Sigma_g\sigma_g \left[\rho_s^{0.5} + \left(\frac{\pi}{4}\rho_g(0)\right)^{0.5} \right].$$



$$P(0) = \rho_g(0)\sigma_g^2 = (2G)^{0.5}\Sigma_g\sigma_g \left[\rho_s^{0.5} + \left(\frac{\pi}{4}\rho_s\right)^{0.5} \right].$$

ρ_s is constant over H_g ?

H_s
 $\gg H_g$ (?)

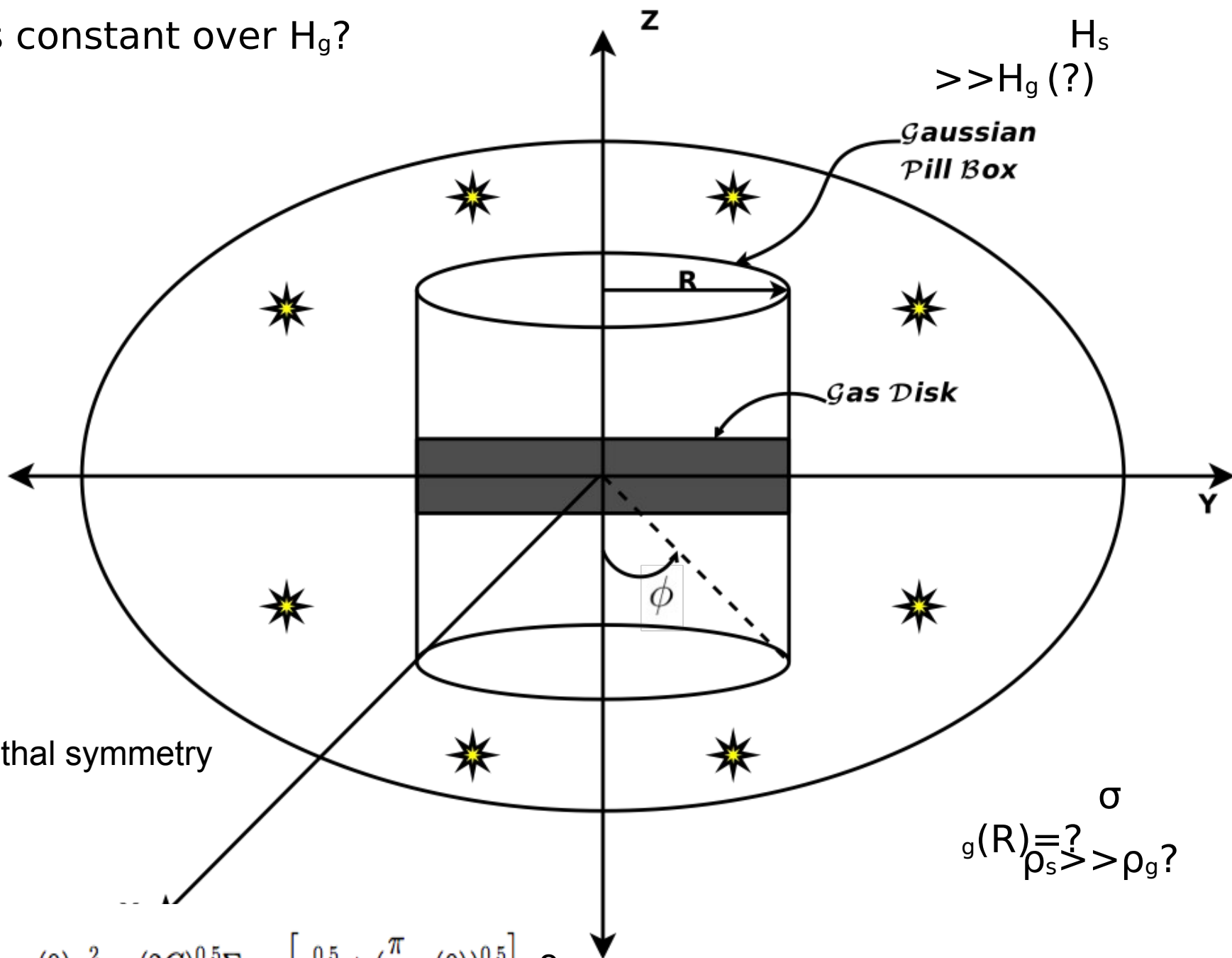
*Gaussian
Pill Box*

Gas Disk

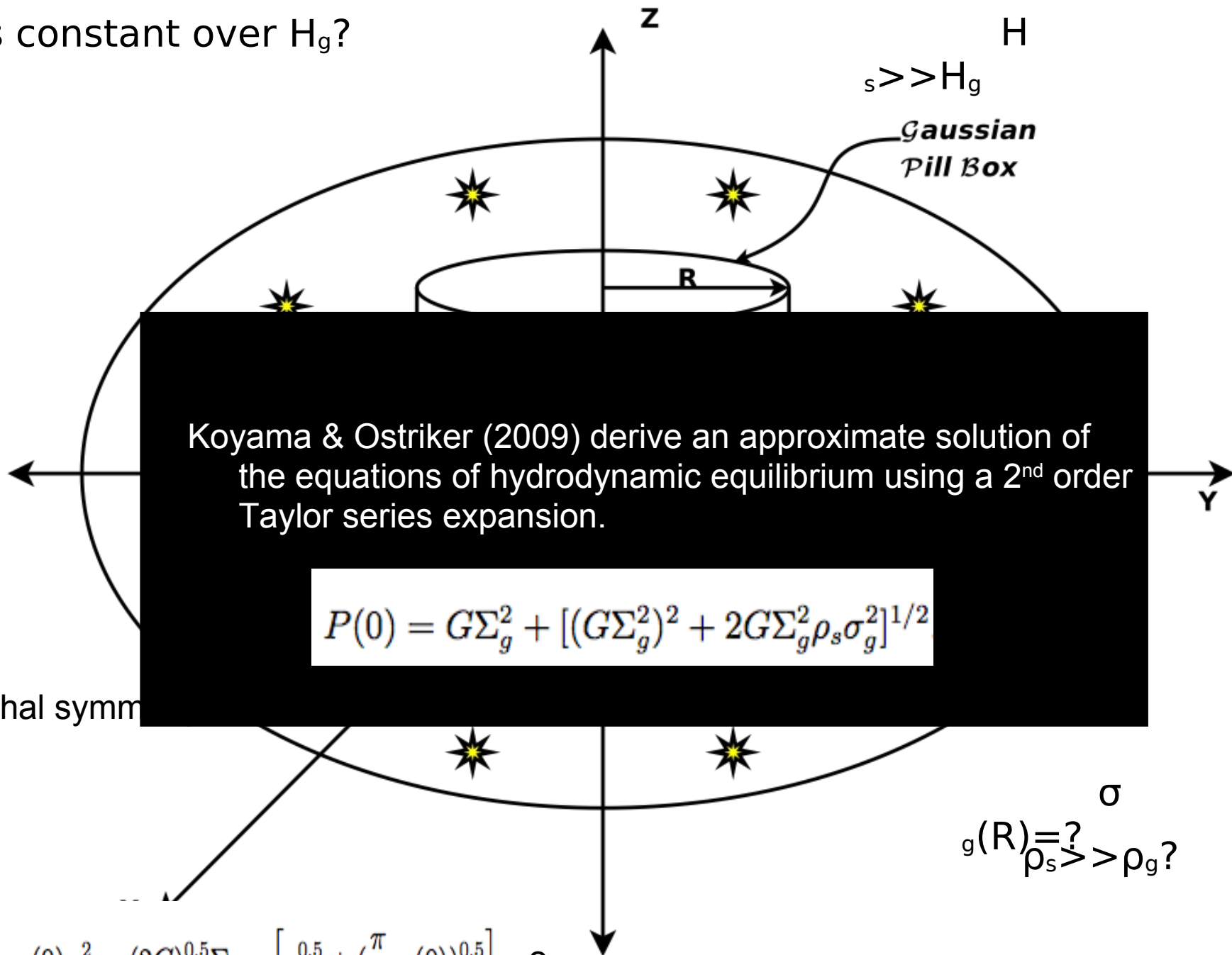
Azimuthal symmetry

σ
 $\rho_s \stackrel{?}{=} \rho_g$
 $\rho_s \gg \rho_g$

$$P(0) = \rho_g(0)\sigma_g^2 = (2G)^{0.5}\Sigma_g\sigma_g \left[\rho_s^{0.5} + \left(\frac{\pi}{4}\rho_g(0)\right)^{0.5} \right]. ?$$



ρ_s is constant over H_g ?



Koyama & Ostriker (2009) derive an approximate solution of the equations of hydrodynamic equilibrium using a 2nd order Taylor series expansion.

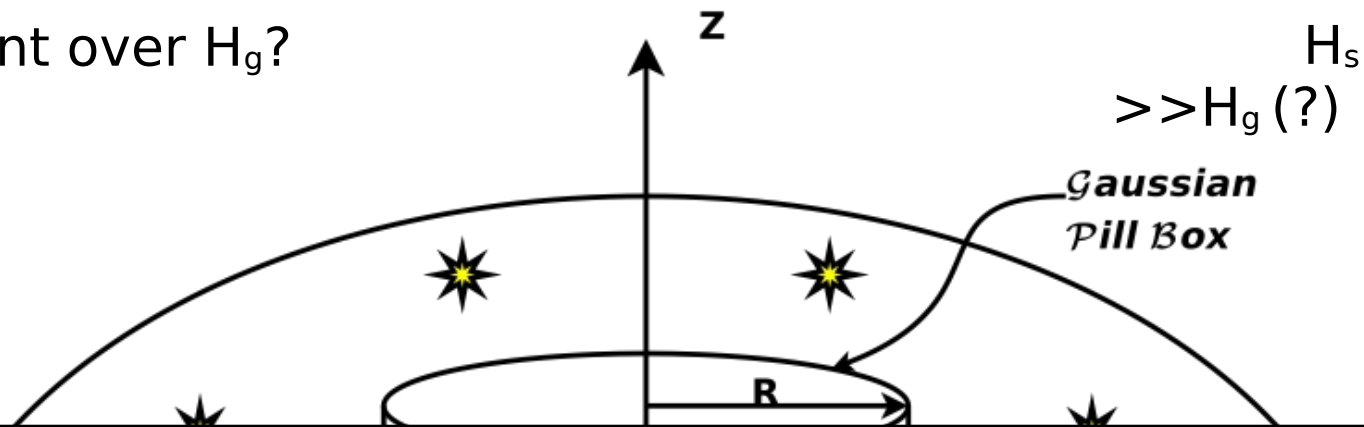
$$P(0) = G\Sigma_g^2 + [(G\Sigma_g^2)^2 + 2G\Sigma_g^2\rho_s\sigma_g^2]^{1/2}$$

Azimuthal symm

$$\rho_s \gg \rho_g \quad \sigma_g(R) \stackrel{?}{=} \sigma$$

$$P(0) = \rho_g(0)\sigma_g^2 = (2G)^{0.5}\Sigma_g\sigma_g \left[\rho_s^{0.5} + \left(\frac{\pi}{4}\rho_g(0)\right)^{0.5} \right]. \quad ?$$

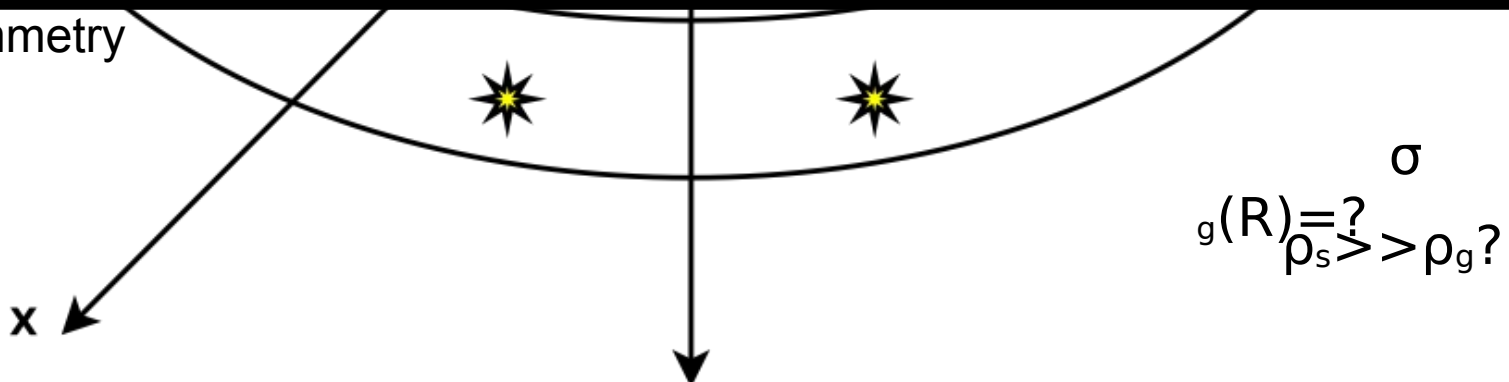
ρ_s is constant over H_g ?



- Numerically this approximate solution gives better estimates than the Blitz & Rosolowsky (2006) formalism.

□ $\rho_g/\rho_s = 4$ produces results only 10% off the "proper" numerical integration whereas the Blitz & Rosolowsky (2006) approximation is off by about 20% to 30%.

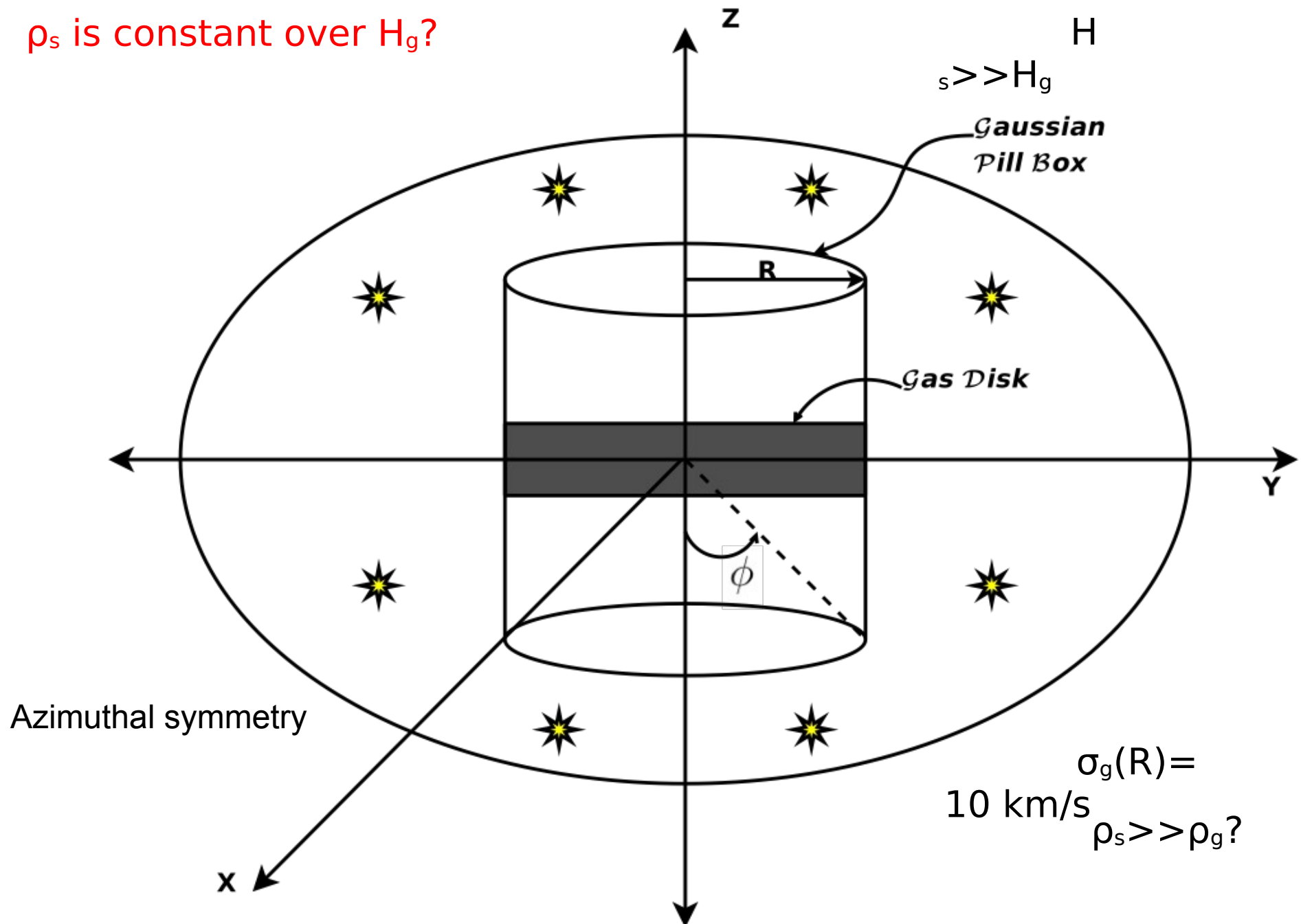
Azimuthal symmetry



$$P(0) = G\Sigma_g^2 + [(G\Sigma_g^2)^2 + 2G\Sigma_g^2\rho_s\sigma^2]^{1/2}$$

Koyama & Ostriker 2009

ρ_s is constant over H_g



$$P(0) = G\Sigma_g^2 + [(G\Sigma_g^2)^2 + 2G\Sigma_g^2\rho_s\sigma_g^2]^{1/2}$$

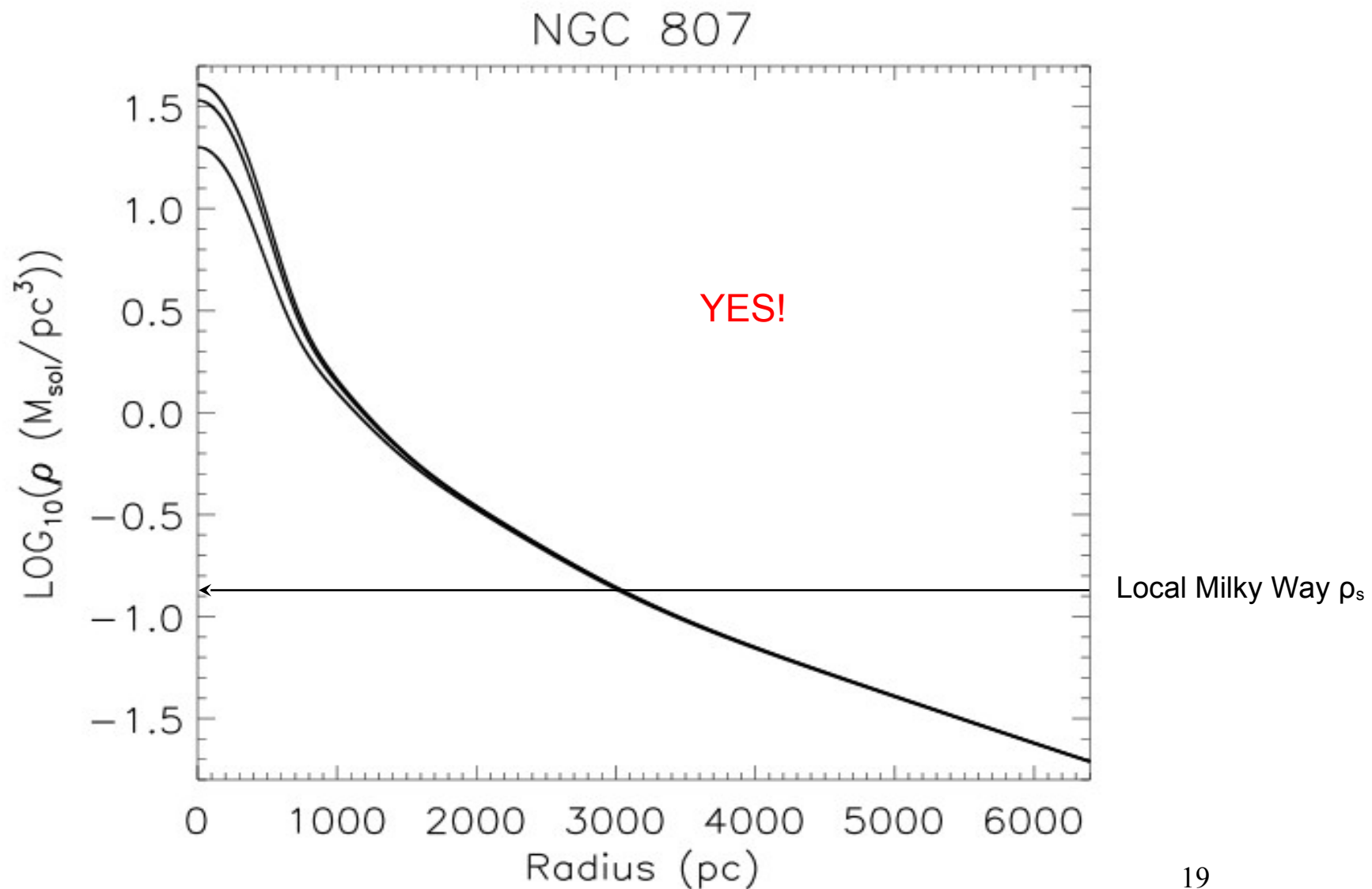
Koyama & Ostriker 2009

Multi-Gaussian (MGE) Stellar Density

- The 3D stellar density, $\rho_s(R,0)$, is determined using a multi-Gaussian expansion (MGE) fit developed by Cappellari (2002) to 2 μ All Sky Survey (2MASS) K_s -band ATLAS images (Skrutskie et al. 2006) or UKIDSS K-band images if available.
 - Characterizes the observed surface brightness as a sum of Gaussians, and allows the photometry to be reproduced in detail.
- Requires an inclination for deprojection.
 - Estimated from optical dust images.
- Requires azimuthal symmetry.
 - Most of the early-type sample galaxies are oblate/fast rotators.
- Doesn't require an assumed stellar scale height.

ρ_s Constant with H_g ?

The MGE stellar density versus radius for several different scale heights.
 $H_s=0$ pc, 150 pc, 300 pc above the midplane.



ρ_s is constant over H_g

H_s
 $\gg H_g$ (?)

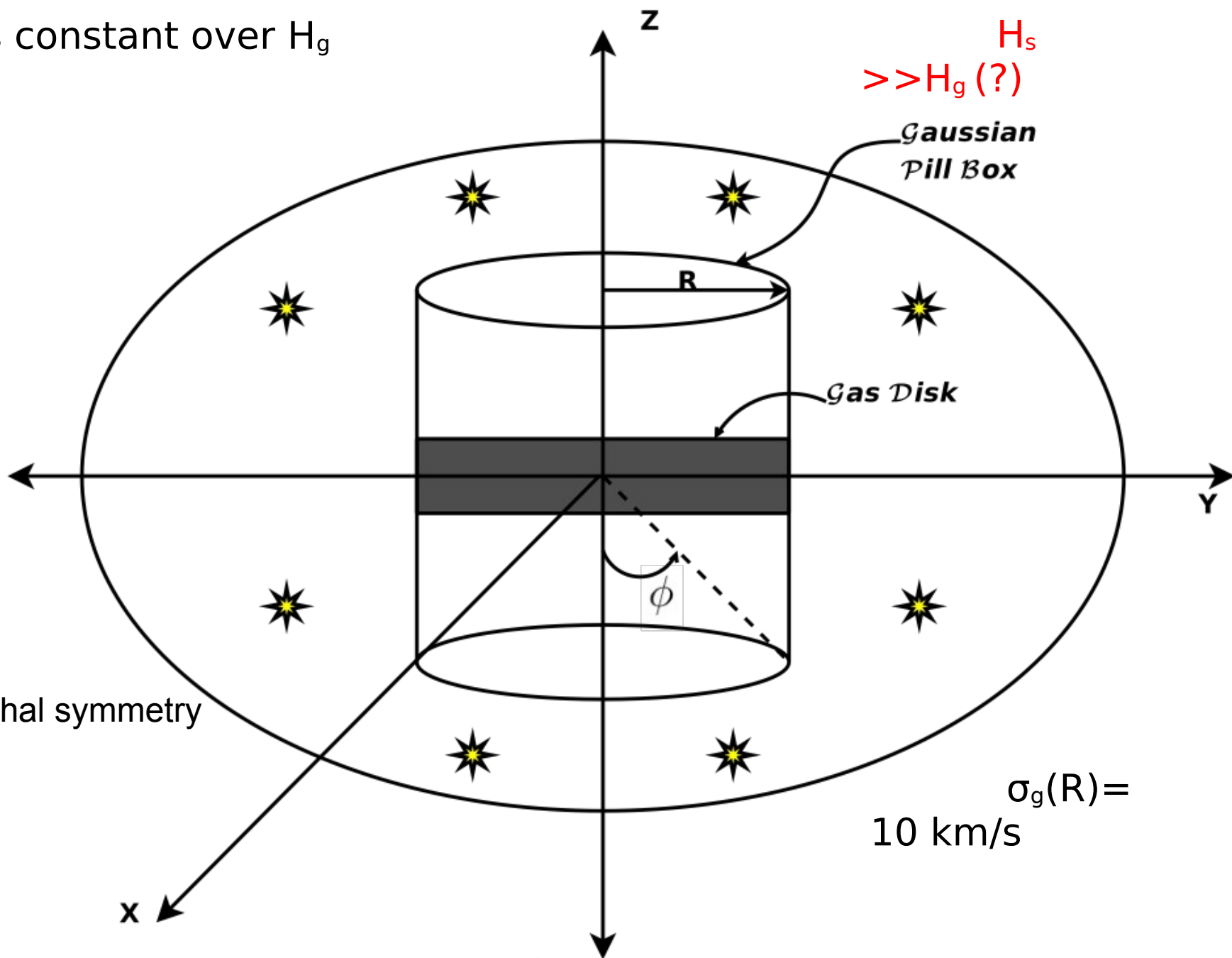
*Gaussian
Pill Box*

Gas Disk

Azimuthal symmetry

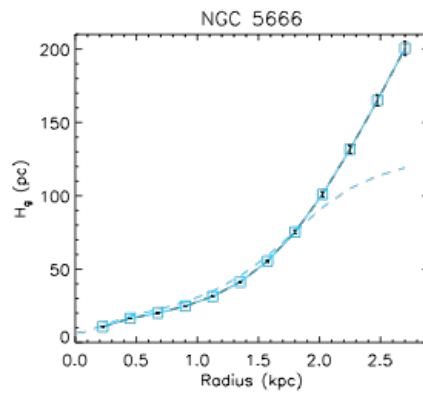
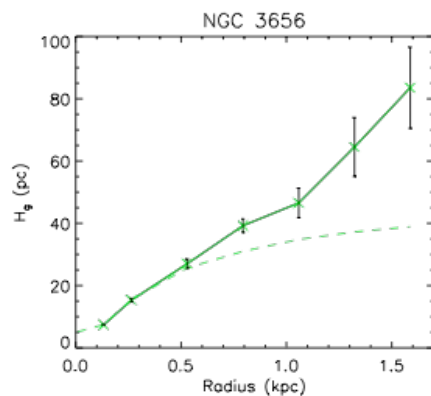
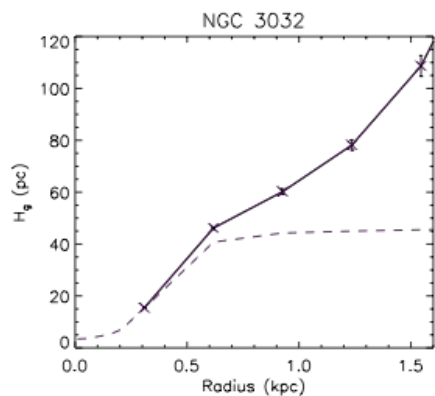
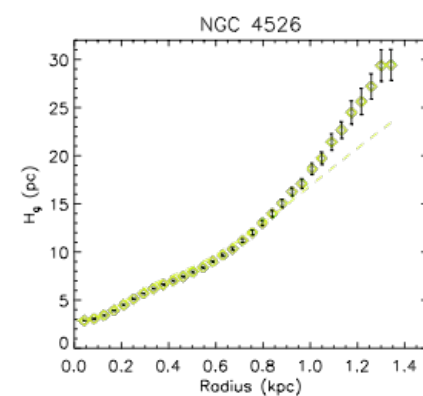
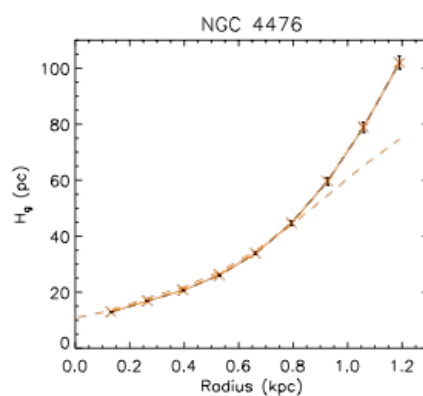
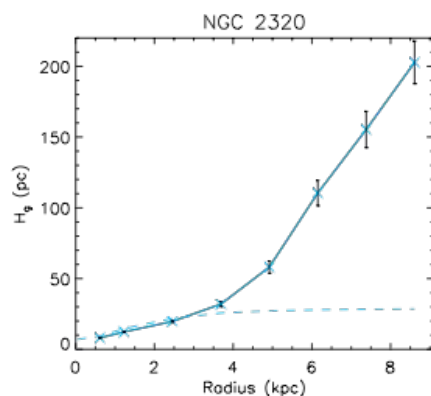
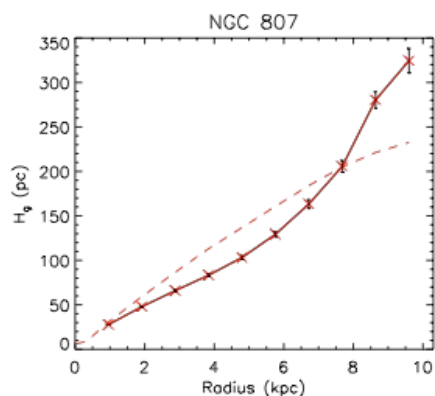
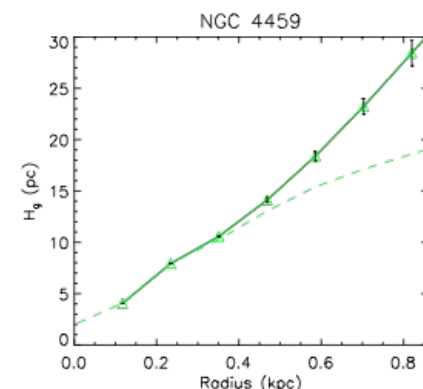
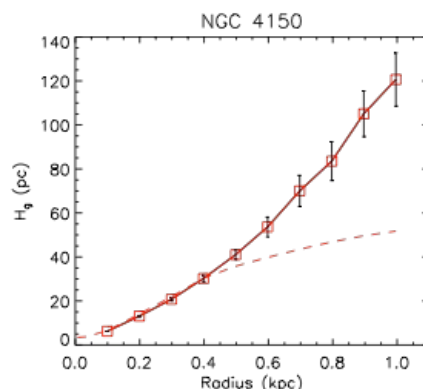
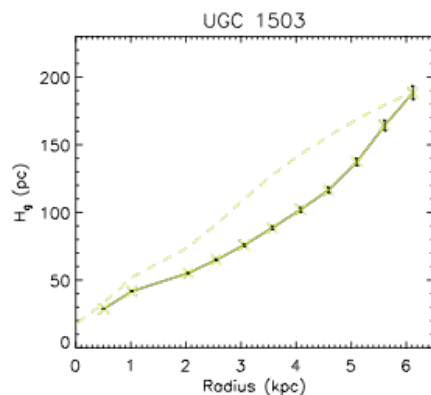
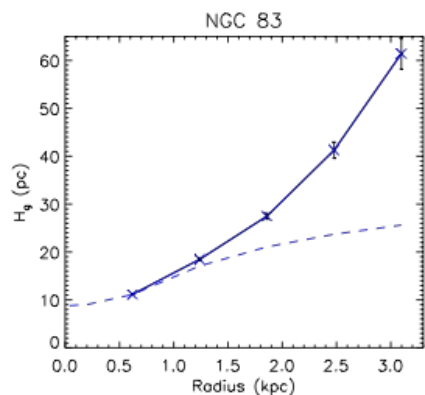
$\sigma_g(R) =$
10 km/s

$$P(0) = G\Sigma_g^2 + [(G\Sigma_g^2)^2 + 2G\Sigma_g^2\rho_s\sigma_g^2]^{1/2}$$



Koyama & Ostriker 2008 ---->

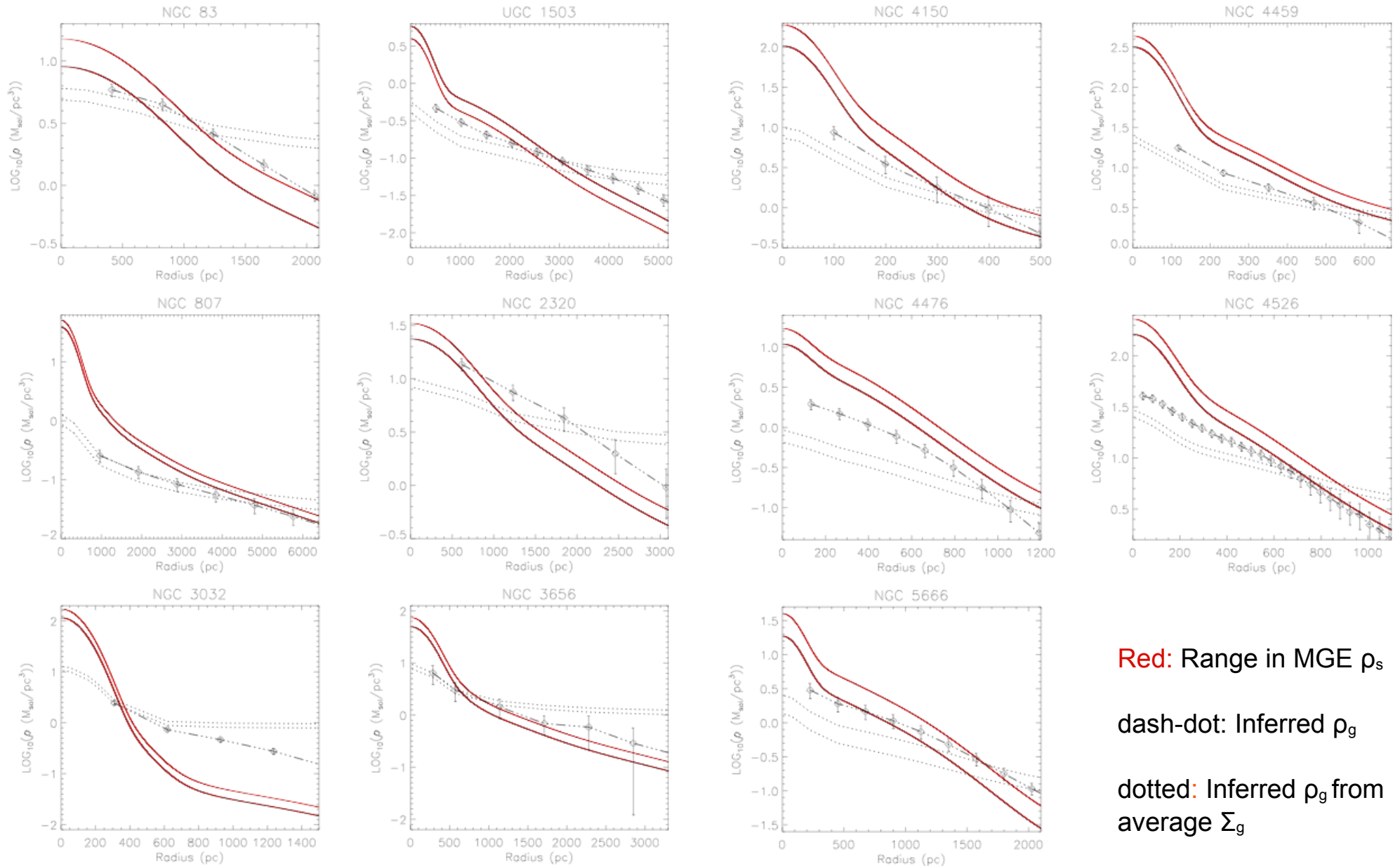
$$H_{est} = \frac{1}{\sqrt{2\pi}} \frac{\sigma_g^2}{G\Sigma_g + [(G\Sigma_g)^2 + 2G\rho_s\sigma_g^2]^{1/2}}$$



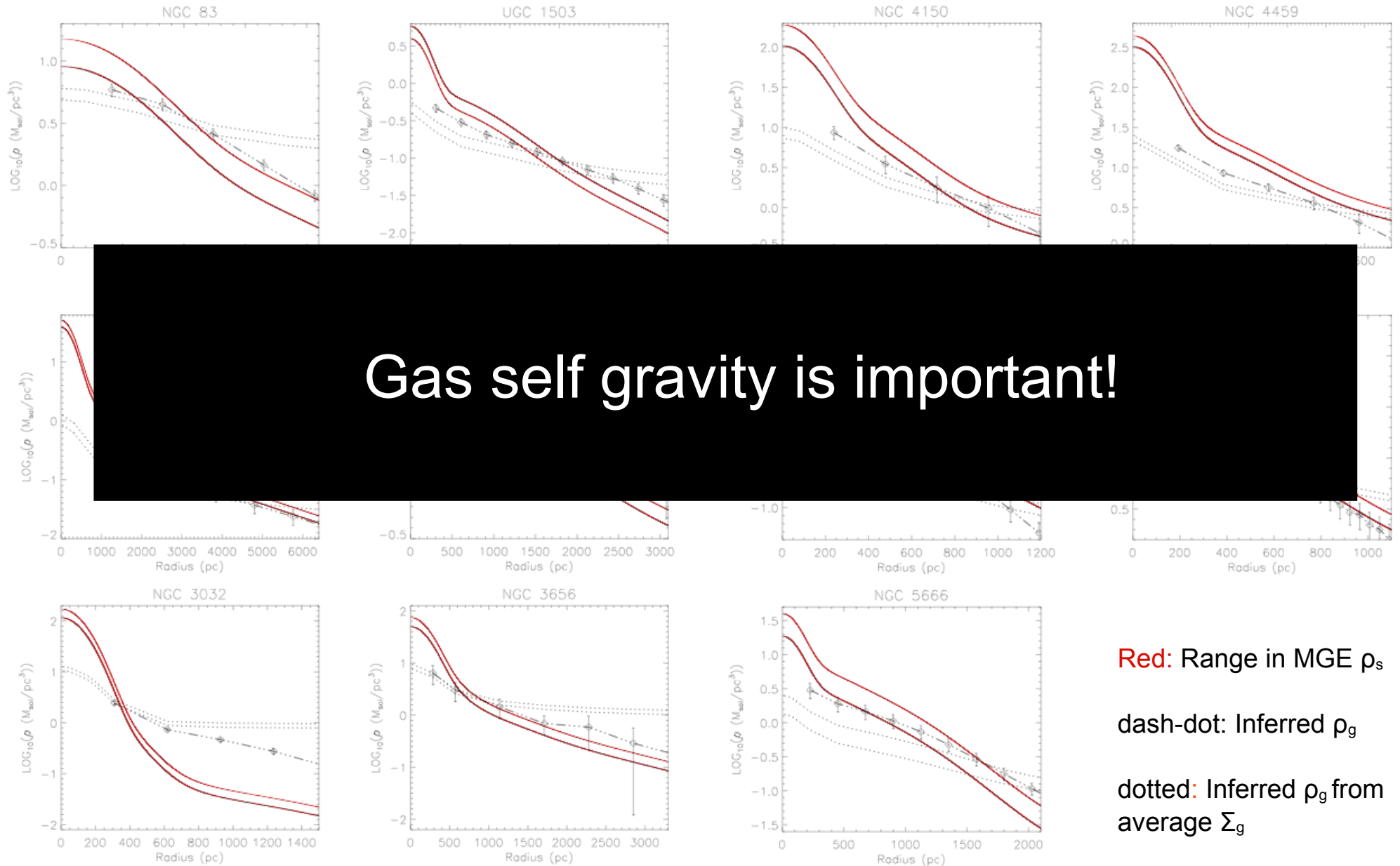
Hg: 5-10 pc in the inner regions to

Hg: 40-340 pc in the outer regions.

$$\rho_g(0) = \frac{G\Sigma_g^2}{\sigma_g^2} + \left(\frac{G^2\Sigma_g^4}{\sigma_g^4} + \frac{2G\Sigma_g^2\rho_s}{\sigma_g^2} \right)^{1/2}$$

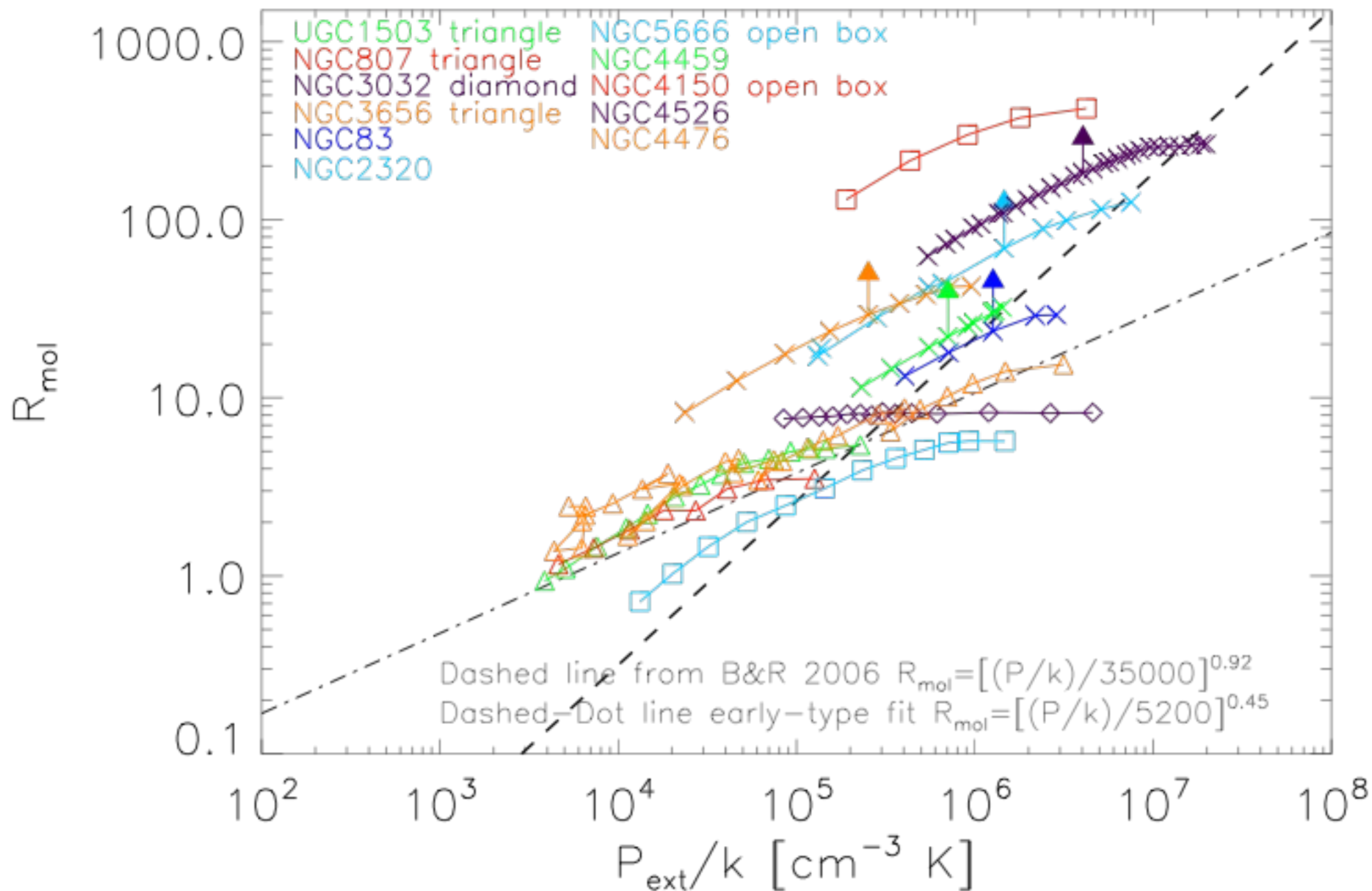


$$\rho_g(0) = \frac{G\Sigma_g^2}{\sigma_g^2} + \left(\frac{G^2\Sigma_g^4}{\sigma_g^4} + \frac{2G\Sigma_g^2\rho_s}{\sigma_g^2} \right)^{1/2}$$



Koyama & Ostriker 2008 ---->

$$P(0) = G\Sigma_g^2 + [(G\Sigma_g^2)^2 + 2G\Sigma_g^2\rho_s\sigma_g^2]^{1/2}$$



R_{mol} -Pressure Relation

- Early-type empirical result: $P = [(P/k_B)/5200 \pm 400 \text{ K cm}^{-3}]^{0.45 \pm 0.09}$
- The Elmegreen (1993) prediction, $F_{\text{mol}} \approx P^{2.2} j(Z)^{-1}$, is only good for $R_{\text{mol}} < 1$
- Krumholz et al. (2009) models recover the observed correlation between R_{mol} and midplane pressure. However they note that their model predictions are only upper limits for $R_{\text{mol}} < 1$. Limiting their synthetic model data and the observed data sets to this parameter space $R_{\text{mol}} > 1$ results in a much more shallow fitted slope.
 - Model data fit for combined B&R06+L08: $R_{\text{mol}} = [(P/k_B)/83 \text{ K cm}^{-3}]^{0.47}$
 - B&R06 data: $R_{\text{mol}} = [(P/k_B)/120 \text{ K cm}^{-3}]^{0.51}$
 - L08 data: $R_{\text{mol}} = [(P/k_B)/83 \text{ K cm}^{-3}]^{0.53}$

R_{mol} -Pressure Relation

• Early-type empirical result: $P = [(P/k_B)/52 \pm 4 \text{ K cm}^{-3}]^{0.45 \pm 0.09}$

• The

• Suggests F_{mol} -Pressure relation has different slope in different regimes?

• Kr

and

only

data

slo

- $R_{\text{mol}} = P^{0.5}$ for $R_{\text{mol}} > 1$

- $R_{\text{mol}} = P^{1.2}$ for $R_{\text{mol}} < 1$

• Model data fit for combined B&R06+L08: $R_{\text{mol}} = [(P/k_B)/83 \text{ K cm}^{-3}]^{0.47}$

• B&R06 data: $R_{\text{mol}} = [(P/k_B)/120 \text{ K cm}^{-3}]^{0.51}$

• L08 data: $R_{\text{mol}} = [(P/k_B)/83 \text{ K cm}^{-3}]^{0.53}$

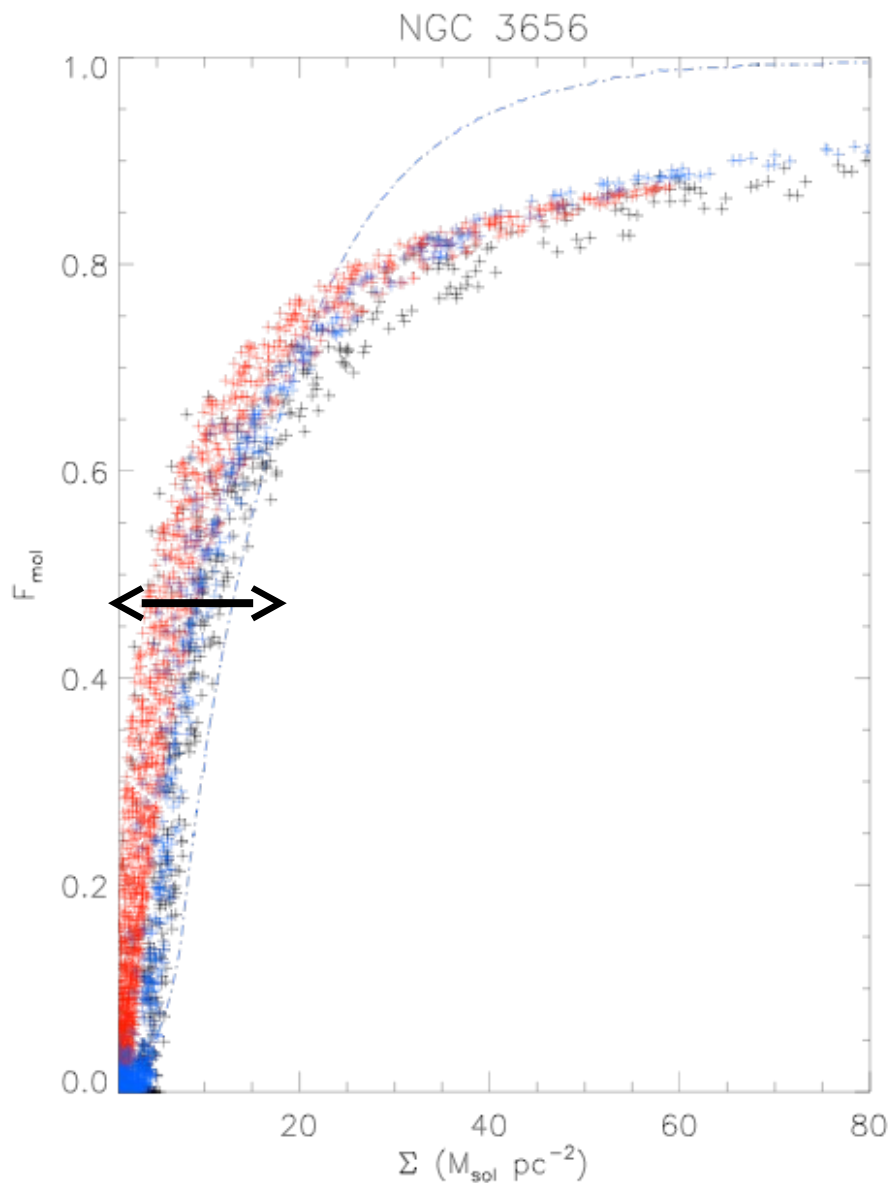
Summary

- Observed HI surface density saturation and total surface density at the transition region are similar to that of early-type galaxies.

- The cold gas systems of CO-rich early-type galaxies fundamentally resemble that of normal spiral galaxies!

- R_{mol} is a much more shallow function of hydrostatic midplane pressure than observed for disk galaxies.

The Molecular Fraction: Resolution Effects



Black pluses: total gas surface density (correct for inclination and the present of helium)

+ 7 arcsec HI and CO maps

+ HI and CO maps smoothed to 15 arcsec resolution

+ 7 arcsec CO map and HI maps smoothed to 15 arcsec

Dash-dot line: Elmegreen 1993 photo-dissociation model with $U_0 = Z_0 = 1$

Robust to Resolution!